Preparation of Reactive and Thermal Stable Hyperbranched Graft Copolymers/ Clay Nanocomposite via 'Living' Free Radical Polymerization

M. Abbasian*, M. Jaymand, M. Z. Ghadami, A. Fathi

Lab. of Polymer, Faculty of Chemistry, Payame Noor University, Tabriz, I. R. Iran

(*) Corresponding author: m_abbasian@pnu.ac.ir

Abstract:

Exfoliated poly (Chloromethyl styrene-co-styrene)-g-polyacrylonitryle/organo- modified montmorillonite [P(CMSt-co-St)-g-PAN/O-MMT] nanocomposite was synthesized through solution intercalation method by using atom transfer and nitroxide mediated radical polymerization. At first, poly (chloromethyl styrene-co-styrene) copolymer was synthesized by nitroxide - mediated "living" free radical polymerization (NMRP). This chlorinated copolymer used as a macro initiators for atom transfer radical polymerization (ATRP). These macro initiators were polymerized acrylonitryle monomers in the presence of CuCl as a catalyst and the 2, 2' – bi pyridine (bpy) as a legend in the tetrahydrofurane (THF) solvent at 90°C. Organophilic montmorillonite (O-MMT) was obtained after treating by hexadecyl trimethyl ammonium chloride salt by ion-exchange process. Finally, (PCMSt-co-PSt)-g-PMMA / O-MMT nanocomposite was prepared by solution intercalation method. The exfoliating structure of nanocomposite was probed by X-ray diffraction (XRD) and scanning electron microscopy (SEM).

Keywords: *Thermal stability, Hyperbranched copolymers, Atom transfer radical polymerization, Clay, Nanocomposite.*

1. INTRODUCTION

In polymer/nanoclay nanocomposites (PNCs), a few weight percent of each silicate layer of clay mineral is randomly and homogeneously dispersed on a nanometer level in the polymer matrix. When molded, the mechanical, thermal, and barrier properties of PNC are superior to those of pristine polymers and/or conventional composites. PNC was firstly invented at Toyota Central R&D Labs [1-3]. Presently, development has widened into almost every engineering polymer including starch [4], polymethylmethacrylate, ethylene-vinyl acetate copolymer [5], polyurethane [6], polypropylene, polyethylene, polystyrene, acrylonitrile butadiene styrene polymer polyacrylonitrile, polycarbonate, polyethylene oxide, epoxy resin, polyimide, polylactide, phenolic resin, polypyrrole, rubber, and polyvinylpyridine [7]. The preparation of a nanocomposite may be accomplished either by an in-situ polymerization or by blending with melt and solution blending=[8-11]. Nanoclay based nanocomposites are described according to the dispersion of the clay in the polymer. In order to form a nanocomposite, the clay must be uniformly distributed. If this uniform distribution is not achieved, the material will be described as a microcomposite or as an

168

immiscible nanocomposite. In an immiscible nanocomposite the clay is not well-dispersed and it is acting as conventional filler. When the clay is well-dispersed, two different types of nanocomposites may be obtained, intercalated and exfoliated nanocomposites. It is generally accepted that delamination is required for enhanced permeability and mechanical properties while the type of the nanocomposite, intercalated or delaminated, does not seem to be important for thermal properties and fire retardancy of polymer materials [12, 13].

Graft copolymers have been extensively studied and have industrial applications. For example, they are used as adhesives, surfactants, thermoplastic elastomers, compatibilization agents in polymer blends, and additives in high-impact materials. In general, graft copolymers can be synthesized by free radical-induced grafting processes, which are the easiest and widely accepted procedures [14]. However, one of the major limitations of this technique is the formation of unwanted homopolymer, which usually proceeds in parallel with the graft copolymerization. In addition, the free radical technique produces many radicals simultaneously, which leads to complex reactions, including chain transfer and chain termination reactions. Therefore, there is a lack of control over molecular weight and polydispersity of the graft chains [15-17]. These problems can be circumvented through applying the atom transfer radical polymerization (ATRP) and nitroxide mediated living free radical polymerizatiopn techniques [18-20].

In this study, we prepared reactive and thermal stable hyperbranched graft copolymers/ clay nanocomposite by solution method and living free radical polymerization. ATRP is used to synthesize graft copolymer on the backbone of poly chloromethyl styrene with functional acrylonitryle monomers and narrow molecular weight distributions. The structure of the resulting nanocomposites was examined with X-ray diffraction (XRD) and scanning electron microscopy (SEM) in particular, the thermal behavior was observed.

2. EXPERIMENTAL

2.1. Materials

TEMPO iniferter were prepared by the method reported by our research group previously [16-19]. Styrene, *p*-chloromethyl styrene and acrylonitrile (Merck) were distilled under reduced pressure. Benzoyl peroxide (BPO) was obtained from Merck and purified by reprecipitation from chloroform into methanol. Toluene and THF (Merck) were dried by refluxing over sodium and distilled under argon prior to use. 2, 2'- bipyridine (Merck) was used as received. Copper (I) chloride (Merck) was purified by stirring in glacial acetic acid, then washed with methanol, and finally dried under reduced pressure. Hexadecyl trimethyl ammonium chloride salt was obtained from Merck. Sodium montmorillonite (MMT) was obtained from Southern Clay Products (USA), under the trade name of Cloisite NaC. MMT is reported to have an approximate aspect ratio of 250:1, and is a 2:1 tetrahedral/octahedral aluminum silicate smectite mineral with an idealized chemical formula of $Na_{0.33}[Mg_{0.33}Al_{11.67} Si_4O_{10}](OH)_2$ and a cation exchange capacity of 95 meq/100 g. All other reagents were purchased from Merck.

2.2. Instrumentation

^{1}H NMR spectra were recorded at 25°C by FT-NMR (400 MHz) Brucker spectrometer. Sample for ^{1}H NMR spectroscopy was prepared by dissolving about 10 mg of products in 5 mL of deuterated chloroform. FT-IR spectra were recorded using Shimadzu FT-IR 8101M. XRD spectra were obtained by using a Siemens D 5000, X-ray generator (CuK$_a$ radiation with λ=1.5406 Å) with a 2θ scan range of 2 to 80° at room temperature. The dispersion state and layered structure of the MMT were observed by using a VEGA//TESCAN, KX5000 SEM (USA). The thermal properties of samples were performed with a TGA- PL (England). Sample of about 10 mg were heated from 25- 600°C at the rate of 10°C min^{-1} under nitrogen flow. Differential scanning calorimetry (DSC) analyses were performed on a Mettler 4000 TA thermal analytical system DSC analyses were carried out using a NETZSCH (Germany) - 200 F3

Maia DSC. The sample was first heated up to 200°C and kept for 5 min to eliminate the heat history. Then it was cooled down at a rate of 10°C/min. After that it was reheated up to 200°C at a rate of 10°C/min. The entire test was performed under the nitrogen purging at the rate of 50 mL min^{-1}.

2.3. Synthesis of poly (chloromethyl styrene-co-styrene) via NMRP

A 100 mL three-necked flask containing 10 mL styrene and *p*-chloromethyl styrene (50/50 v/v) and 0.15 g (0.7 mmol) benzyl peroxide and 0.13 g (90 mmol.Lit^{-1}) TEMPO stirred at 95°C for 4 h under argon atmosphere. Then the temperature was increased up to 130°C and mixture stirred for another 12 h. The mixture was cooled at room temperature and polymer was recovered by filtration in ice methanol. This product was dried overnight in vacuum at room temperature.

2.4. Synthesis of poly (chloro methyl styrene-co-styrene) -grafted acrylonitrile

In a typical experiment, a dry round-bottomed flask fitted with magnetic stirring bar was charged with THF (20 mL), CuBr (0.07 g, 0.48 mmol), bpy (0.15 g, 0.96 mmol), acrylonitrile (5 g), and poly choloromethylstyrene-*co*-styrene (1 g). The flask was sealed and three cycles of freeze-pump-thaw were performed to remove oxygen. Then the flask was filled with purified nitrogen. After which the reaction mixture was heated at 90°C and maintained at this temperature for 12 h with stirring. The reaction was terminated by pouring the content of the flask into a large amount of methanol. This product was dried overnight in vacuum at room temperature.

2.5. Removal of the copper contaminants

The crude product was greenish in color due to copper residues retained. To remove the copper contaminants from the crude product, the powder was extracted with acetylacetone–ethanol solution (100 mL, vol. ratio of 1:5) for 24 h. The product was filtered and washed with ethanol and excess of water in turn. In this way, almost white powders were obtained.

2.6. Surface modification of montmorillonite

Organophilic montmorillonite (O-MMT) was obtained after treated with hexadecyl trimethyl ammonium chloride salt ion-exchange process. Montmorillonite was first dispersed in deionized water under ultrasound for 1 h (UNICOM INSTRUMENTS, USA). The modifier was prepared in deionized water separately, and was added to the clay dispersion at an amount a little higher than the CEC of montmorillonite. The resulted suspension was intensively stirred for 10 h, and was then filtered and washed with deionized water three times. The final product was dried in vacuum oven at room temperature for 48 h and grounded into powder.

2.7. Preparation of polymer/organoclay nano-composite

Certain amount of organophilic montmorillonite (3 Wt %) was first dispersed in 30 mL carbon tetrachloride under ultrasound for 30 min. Then certain amount (1 g) of (PCMSt-*co*-PSt)-*g*-PAN dissolved in 50 mL carbon tetrachloride. The clay suspension was then slowly added to the polymeric solution under vigorously stirring. The resulted suspension was intensively stirred for 6 h at 60°C. Then the mixture was poured into methanol for rapid precipitation. The precipitate was filtered and dried at 50°C under vacuum for 2 days.

3. RESULTS AND DISCUSSION

3.1. Synthesis of poly (chloromethyl styrene-co-styrene) via NMRP

Living polymerization is characterized by a linear increase of the molecular weight with conversion and reaction time, and a narrow molecular weight distribution as evidenced by a polydispersity index (PDI=Mw/Mn) approaching 1 [21]. Figure 1 represents the GPC chromatograms of the poly
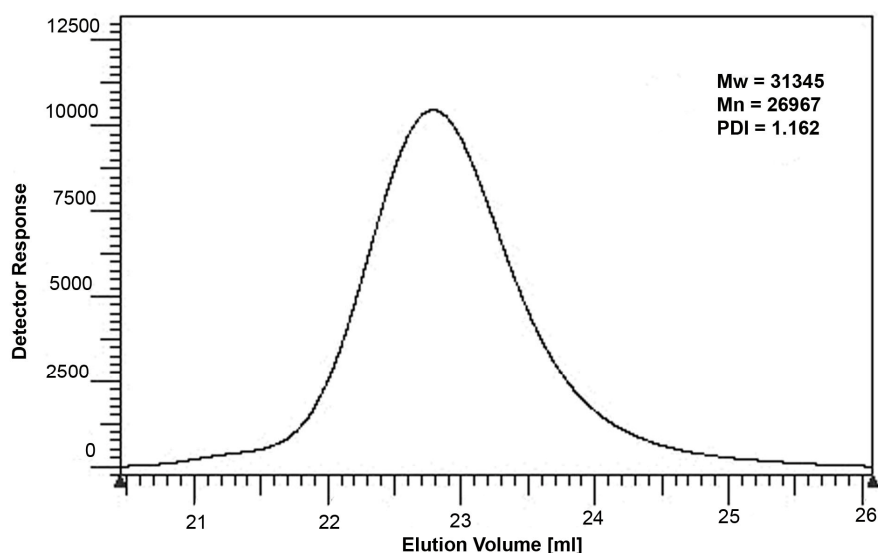
Figure 1: *GPC chromatograms of poly (chloro methylstyrene-co-styrene) copolymer*

(chloro methylstyrene-*co*-styrene) copolymer whose molecular weight distribution by GPC is 1.162. The single peak of the GPC curve of the product indicated that the product could not be the blend of PCMSt homopolymer and PSt homopolymer; if so, the GPC curve should appear as two peaks, one for the PCMSt homopolymer and the other for the PSt homopolymer.

The ^{1}H NMR of poly (chloromethyl styrene-*co*-styrene) copolymer is shown in Figure 2. The ^{1}H NMR spectra shows the resonance at about 1.09-2.34 ppm which is assigned to the aliphatic protons in copolymer and resonance at about 6.08-7.54 ppm which are assigned to aromatic protons. Also the ^{1}H NMR spectra shows the resonance at about 4.12-

4.63 ppm that is assigned to the CH$_2$-Cl group in poly chloromethyl styrene unite.

To calculate the extent of chlorine in copolymer the following method was adopted. Let $(PSt)_m$–$(PCMSt)_n$ represent the chlorine in copolymer. The mol % chlorine unite in copolymer is given by $n/(m+n) \times 100$. The area under the aliphatic region is given by $8n+5m$ and the area under the aromatic region is given by $9n+9m$. In Figure 2 by solving the simultaneous equation with the integrated areas, it can be seen that $8n+5m=0.3623$ and $9n+9m=0.4958$ and therefore $n=0.0291$ and $m=0.0259$. Therefore the extent of chlorine is $0.0291/0.055 \times 100 = 52.9\%$.
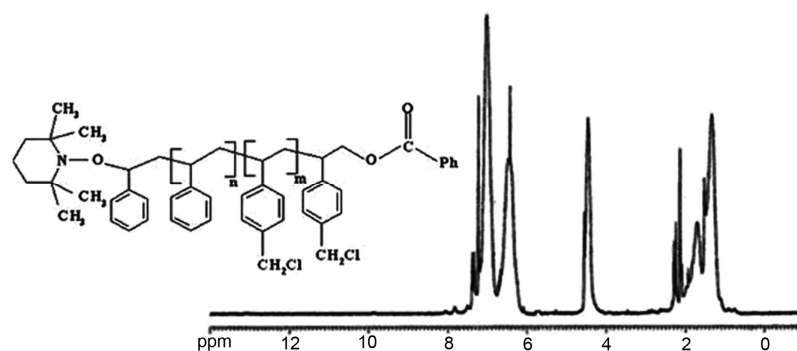

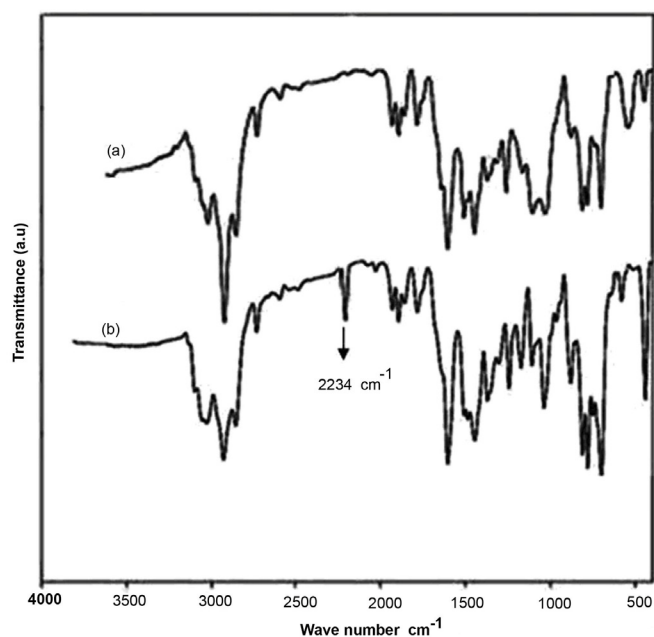**Figure 2:** *^{1}H NMR spectra of poly (chloromethyl styrene-co-styrene)*

Figure 3: *FT-IR spectra of the poly (chloro methylstyrene-co-styrene) copolymer (a) and poly (chloro methylstyrene-co-styrene)-grafted acrylonitrile (b)*
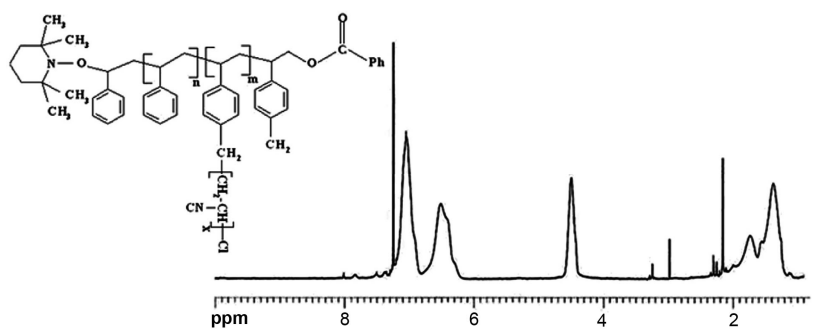

Figure 4: *^{1}H NMR spectra of poly (chloromethyl styrene-co-styrene)-grafted acrylonitrile*
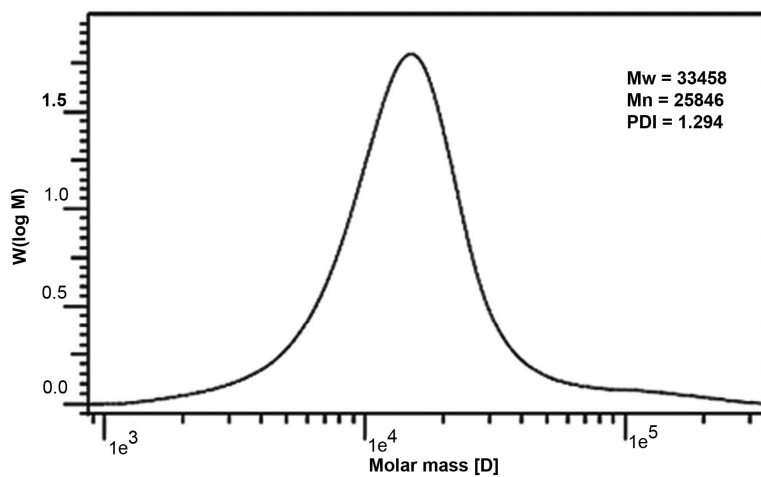

Figure 5: *GPC chromatograms of the poly (chloro methylstyrene-co-styrene)-g- polyacrylonitrile*
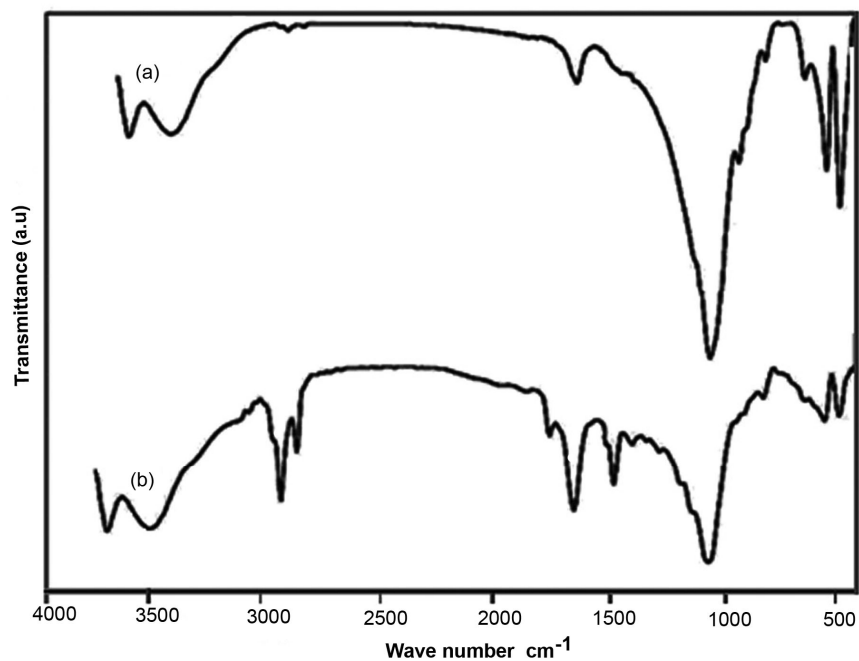
Figure 6: *FT-IR spectra of the unmodified montmorillonite (a) and modified montmorillonite (b).*
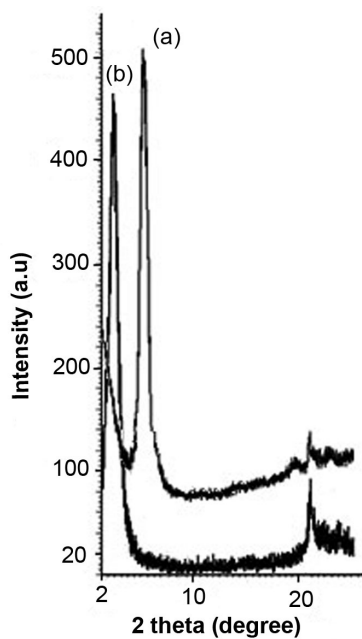

Figure 7: *XRD patterns of the parent montmorillonite (a) and the organomodified montmorillonite (b)*

3.2. Synthesis of poly (cloromethyl styrene-co-styrene)-grafted acrylonitrile via ATRP technique

Figure 3 shows the FT-IR spectra of the poly (chloromethyl styrene-*co*-styrene) copolymer (a) and poly (chloro methyl styrene-co-styrene)-*grafted* acrylonitrile (b). The FT-IR spectra of poly (chloromethyl styrene-*co*-styrene) shows the characteristic absorption bands due to stretching vibration of C-H (3100-2850 cm^{-1}), weak aromatic overtone and combination bands in the 2100-1670 cm^{-1} region, C=C stretching vibrations (1606 and 1485 cm^{-1}), CH$_2$ bending vibrations (1445 and 1372 cm^{-1}), and γ(C-H) in the aromatic ring (768 and 709 cm^{-1}) observed. The absorption band due to C-Cl group observed at 557 cm^{-1}. Figure (3b) exhibit additional absorption band at 2234 cm^{-1} attributed to nitril group in poly (methyl styrene-*co*-styrene)-*grafted* acrylonitrile comparison with poly (methyl styrene-co-styrene) copolymer.

Figure 4 shows the ^{1}H NMR spectra of poly (chloromethyl styrene-*co*-styrene)-*grafted* acrylonitrile. Grafting of acrylonitrile onto poly (chloromethyl
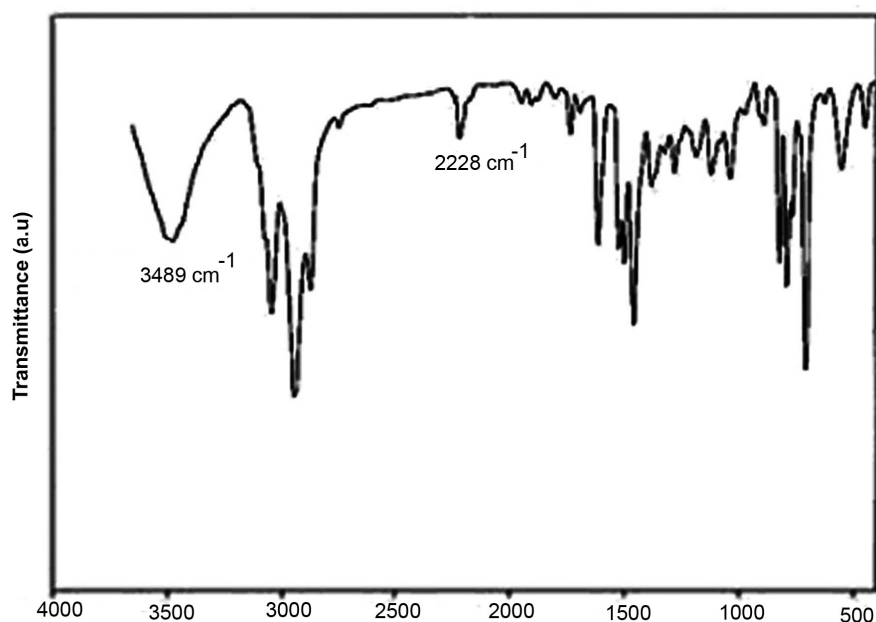
Abbasian, *et al.*   173

Figure 8: *FT-IR spectra of (PCMSt-co-PSt)-g-PAN / O-MMT nanocomposite*

styrene-*co*- styrene) copolymer cause decreased the area under CH_2-Cl resonance from 0.1268 to 0.1061. Calculation the extent of chlorine in poly (chloromethyl styrene-*co*-styrene)- *grafted* acrylonitrile shows that the extent of chlorine is 44.6%. Therefore 15.7 % of CH_2-Cl groups grafted by polyacrylonitrile.

The grafting parameters such as grafting yield, grafting efficiency, and weight gain were calculated, based on the gravimetric measurements, according to the following equations: grafting yield (%G)= $(W_g-W_0)/$ W_g ×100; grafting efficiency (%GE)= $W_g/(W_m+$ $W_0)$ ×100; weight Gain (%WG)=$(W_g-W_0)/(W_m+$ $W_0)$ ×100; where W_g is the mass of the grafting copolymer, W_0 is the mass of polymeric initiator (PCMSt-*co*- PSt), and W_m is the mass of the monomer taken for the reaction. The grafting parameters for poly (chloromethyl styrene-*co*-styrene) grafted acrylonitrile calculated and summarized in table 1.

Figure 5 shows the GPC chromatograms of the poly (chloro methylstyrene-*co*-styrene)-*g*-polyacrylonitrile, whose molecular weight distribution by GPC is 1.294. The single peak of the GPC curve of the product indicated that the product could not be the blend; if so, the GPC curve should appear as two or more peaks.

3.3. Preparation of organophilic montmorillonite

Figure 6 shows the FT-IR spectra of the unmodified montmorillonite (a) and modified montmorillonite (b). In the spectra of both modified and unmodified clays, the intense peak at 1045 cm^{-1} and two bands at 467 and 525 cm^{-1} were assigned to Si-O bonds' stretching and Si-O bonds' bending, respectively. The bands around 1637 and 3630 cm^{-1} are due to the hydroxyl groups in the clay. The other additional

Table 1: *Grafting parameters for (PCMSt-co-PSt)-g-PAN*

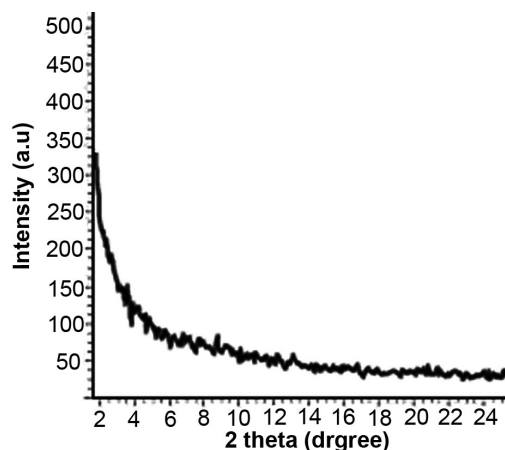| Mass of grafting terpolymer (W_g)	Weight gain(%WG)	Grafting efficiency (%GE)	Grafting yield (%G)
2.38	23	39.67	58

Figure 9: *XRD pattern of (PCMSt-co-PSt)-g-PAN / O-MMT nanocomposite*

bands observed in the spectrum of the modified clays arise from surfactant bonds' stretching or bending. The FT-IR spectra of modified clay exhibits an absorption band at 1467 cm^{-1} attributed to C-H bending bonds. In additionally intercalation of modifier instead of sodium ions can be confirmed by the C-H stretching vibration at 2855 and 2925 cm^{-1}.

Figure 7 shows the XRD patterns of the parent montmorillonite (a) and the organomodified montmorillonite (b). An increase of the basal spacing (d_{001}) of the modified clay is observed after the surfactant insertion. More specifically, the

pristine montmorillonite shows a d_{001}-spacing of 12.6 Å which corresponds to an interlayer space D = 12.6 - 9.6 = 3 Å, where 9.6 Å is the thickness of the individual clay sheet. In the case of the organoclay, the basal spacing d_{001} becomes 18.38 Å, with corresponding interlayer space D = 8.66 Å.

3.4. Preparation of polymer/organoclay nanocomposites

Figure 8 shows the FT-IR spectra of the (PCMSt-*co*-PSt)-*g*-PAN / O-MMT nanocomposite. Apparently the FT-IR spectra of nanocomposite shows the combination of organomodified montmorillonite, (PCMSt-*co*-PSt)-*g*-PAN. The bands around 3489 cm^{-1} are due to the hydroxyl group in the clay and absorption band at 2234 cm^{-1} attributed to nitril group in terpolymer. The other additional bands observed arise from (PCMSt-*co*-PSt)-*g*-PAN stretching or bending bands. FT-IR spectrum assignments verify that the O-MMT layers have been doped into the polymers matrix during the solution intercalation and thus form the (PCMSt-*co*-PSt)-*g*-PAN / O-MMT nanocomposites.

X-ray diffraction, XRD, provides information on the changes of the inter layer spacing of the clay upon the formation of a nanocomposites. The formation of an intercalated structure should result in a decrease in 2θ, indicating an increase in the d-spacing; the formation of an exfoliated structure usually results in
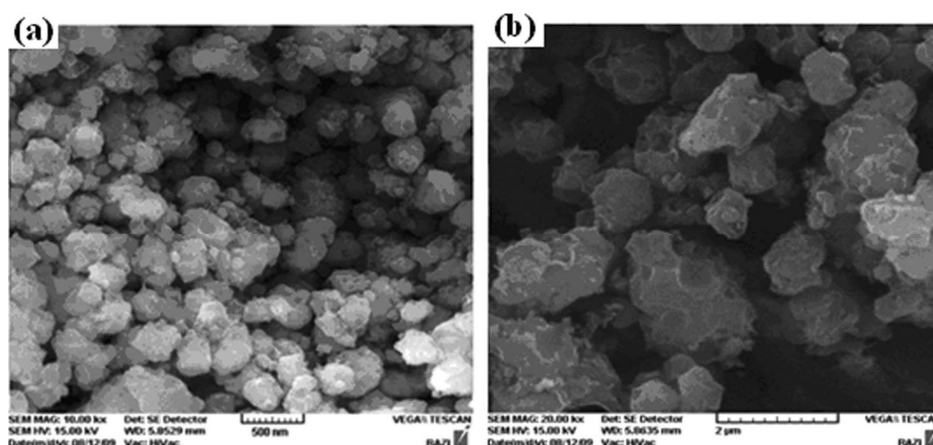

Figure 10: *SEM images for the (PCMSt-co-PSt)-g-PAN / O-MMT nanocomposite*

the complete loss of registry between the clay layers and no peak can be seen in the XRD trace. In some cases, a disordered immiscible system is obtained and this also shows no peaks, so the absence of an XRD peak cannot be taken as definitive evidence for the formation of a exfoliated nanocomposite and additional evidence, usually transmission electron microscopy (TEM) or scanning electron microscopy (SEM), are required. Figure 9 presents the XRD data for the (PCMSt-*co*-PSt)-*g*-PAN / O-MMT nanocomposite. For the nanocomposite no peaks are observed. Nanocomposites, which could mean either that an exfoliated or an immiscible nanocomposite has been formed.

3.5. SEM characterization of nanocomposites

Scanning electron microscope, SEM, provides an actual image of the nanocomposite morphology. Usually both low magnification images, to show if the clay is well-dispersed or not, and high magnification images, to provide an identification of the morphology, are necessary. SEM is complementary to XRD, especially when peaks are not observed in XRD. Figure 10 shows SEM images for the (PCMSt-*co*-PSt)- *g*-PAN / O-MMT (a, b) nanocomposite. The images show that the clay is well-dispersed in the polymeric matrix.

3.6. Glass transition of nanocomposite

Figure 11 shows the DSC traces of the (PCMSt-*co*-PSt) (a), (PCMSt-*co*-PSt)-*g*-PAN (b) and (PCMSt-co-PSt)-*g*-PAN / O-MMT (c) nanocomposite. The (PCMSt-*co*-PSt) exhibits an endothermic peak approximately at 74 °C, corresponding to the glass transition temperature (T_g). In Figure (b) the transition observed at 79 °C can be designed as the glass transition temperature of (PCMSt-*co*-PSt)-*g*-PAN terpolymer. This spectra show the endothermic peaks at 113 °C and 143 °C that has been attributed to the evaporation of any residual water and solvent molecules present in the polymer matrix. A strong exothermic peak appears at 181 °C that indicates the degradation of ungrafted (PCMSt-*co*-PSt). Also strong exothermic peaks appear at 264 °C and 316 °C that indicate the degradation of

(PCMSt-*co*-PSt)-*g*- PAN that low and high grafted PAN respectively. The Tg of the (PCMSt-*co*-PSt)-*g*-PAN / O-MMT nanocomposite (3 Wt% O-MMT) is 84 °C, slightly higher than the (PCMSt-*co*-PSt) and pure (PCMSt-*co*-PSt)-*g*- PAN. In addition, the glass transition temperature (T_g) was also increased slightly in the presence of the clay. The increased T_g resulted from the restricted segmental motion of the polymer chain at the organic-inorganic interface, due to the confinement of the (PCMSt-*co*-PSt)-*g*-PAN chains between the silicate layers, as well as the silicate surface polymer interaction in the nano structured hybrids. This result also indicates nano platelets were reasonably well exfoliated and dispersed. It was also reported in the literature that the majority of the other well-dispersed polymer
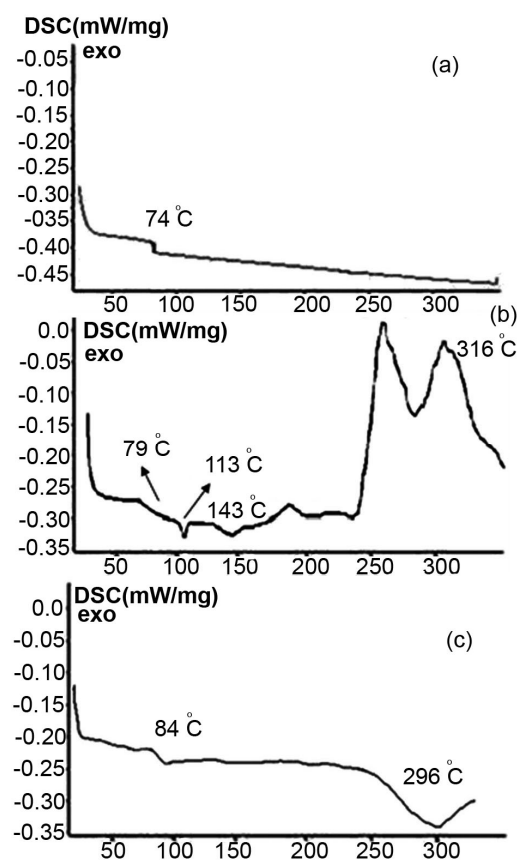

Figure 11: *DSC traces of (PCMSt-co-PSt) copolymer (a), (PCMSt-co-PSt)-g-PAN (b) and (PCMSt-co-PSt)-g-PAN / O-MMT (c)*
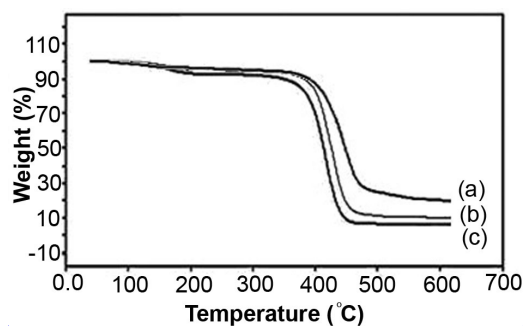
Figre 12: *TGA curves of (PCMSt-co-PSt)-g-PAN / O-MMT (a), (PCMSt-co-PSt)-g-PAN (b) and (PCMSt-co-PSt) copolymer (c)*

nanocomposites also exhibited higher T_g than their corresponding pristine polymer [22].

3.7. Thermal stability of nanocomposite

The thermal stabilities of all the prepared (PCMSt-co-PSt)-g-PAN / O-MMT nanocomposites were higher than those of virgin (PCMSt-co-PSt) and (PCMSt-co-PSt)-g-PAN. The enhancement in thermal stability increased only slightly as the clay loading increased. The improvement in thermal stability of polymereclay nanocomposites is explained by the formation of clay char which acts as the mass transport barrier and insulator between the polymer and the superficial zone where the polymer decomposition takes place. The thermal stability has been also attributed to restricted thermal motions of the polymer localized in the galleries.

4. CONCLUSIONS

Poly (chloromethyl styrene-*co*-styrene) copolymer was synthesized by nitroxide - mediated "living" free radical polymerization (NMRP). This founctionalized copolymer used as a macro initiators for atom transfer radical polymerization (ATRP). These macro initiators can polymerize acrylonitryle monomers in the presence of CuCl as a catalyst and the 2, 2' – bipyridine (bpy) as a legend. Exfoliated P(CMSt-*co*-St)-*g*-PAN / O-MMT nanocomposite was synthesized through solution intercalation method. The exfoliating structure of nanocomposites was probed by XRD and SEM. Also the structure of obtained copolymer, therpolymers and all the components were investigated by ^{1}H NMR, GPC and FT-IR spectroscopy and their thermal behavior were examined by DSC and TGA analyses. TGA results indicate that the improvement of the thermal stability of nanocomposite is comparable to (PCMSt-*co*-PSt) copolymer and graft terpolymer.

5. ACKNOWLEDGMENT

REFERENCES

1. A. Okada, A. Usuki, Mater. Sci. Eng. C, 3 (1995): 109.

2. V. Khrenov, F. Schwager, M. Klapper, M. Koch, K. Müllen, Polymer Bulletin. 58, (2007): 799.

3. A. Ravishankar, L. Arkady, Polymer Bulletin. 43(3) (2004): 292.

4. L. Wenhua, Z. Guangjie, Polymer Bulletin. 6(1) (2004): 54.

5. S. T. Lim, Y. H. Hyun, C. H. Lee, H. J. Choi, Polymer Bulletin. 22(4) (2003): 299.

6. H. C. Kuan, W. P. Chuang, C. M. Ma, C. L. Chiang, H. L. Wu, Polymer Bulletin. 40(1) (2005): 179.

7. D. Wang, C. Wilkie. Polymer Bulletin. 143 (2007): 287.

8. A. B. Morgan, J. D. Harris, Polymer 45 (2004): 8695.

9. A. Samakande, P. C. Hartmann, V. Cloete, R. D. Sanderson, Polymer. 48 (2007): 1490.

10. E. Giannelis, Adv. Mater. 8 (1996): 29.

11. J. W. Gilman, C. L. Jakson, A. B. Morgan, R. H. Harris, E. Manias, E. P. Giannelis, Chem. Mater. 12 (2000): 1866.

12. Y. Wang, F. B. Chen, Y. C. Li, K. C. Wu, Annu. Tech. Conf. Soc. Plast. Eng. 61 (2003): 3670.

13. S. Su, D. D. Jiang, C. A. Wilkie, Polym. Degrad. Stab, 83 (2004): 321.

14. J. Xia, K. Matyjaszewski, Macromolecules. 30 (1997): 7697.

15. M. Abbasian, A. Entezami, Iranian Polymer Journal. 15 (2006): 395.

16. P. Shoaeifar, M. Abbasian, A. Entezami, Journal of Polymer Research. 14 (2007): 45.

17. M. Abbasian, H. Namazi, A. Entezami, Polym. Adv. Technol. 15 (2004): 606.

18. A. Entezami, M. Abbasian, Iranian Polymer Journal. 15 (2006): 583.

19. M. Abbasian, S. Rahmani, R. Mohammadi, A. Entezami, Journal of Applied Polymer Science. 104 (2007): 611.

20. H. Gheybi, M. Abbasian, P. Najafi Moghaddam, A. Entezami, Journal of Applied Polymer Science. 106 (2007): 3495.

21. G. Moad, E. Rizzardo, S. H. Thang, Aus. J. Chem. 58 (2005): 379.

22. Y. Li, B. Zhao, S. Xie, S. Xharng, Polym. Int. 52 (2007): 892.